Chapter 2
A Complex Model of Snake Robot Locomotion on Planar Surfaces

The underlying theme of this book is analytical approaches aimed at increasing our understanding of snake robot locomotion. The mathematical model of the snake robot is the basis for these analytical studies, which means that the analysis relies heavily on the form and complexity of the model. In this chapter, we employ first principles to derive a mathematical model of the kinematics and dynamics of a snake robot with N links moving on a horizontal and flat surface. The links of the robot are influenced by ground friction forces which propel the motion. Due to the many degrees of freedom of the robot and the dynamical couplings between the links, the resulting model will turn out to be quite complex. We will eliminate some of this complexity by partially linearising the model. This is achieved by introducing a change of coordinates which enables us to partition the model into an actuated part (the joint angles of the snake robot) and an unactuated part (the position and orientation of the snake robot). Through an input transformation, we are then able to linearise the actuated part of the model. However, even the partially linearised model contains complex terms which make model-based controller design and analysis challenging. Throughout this book, we will therefore refer to the model developed in this chapter as the *complex* model of the snake robot.

In Chap. 4, the complex model will be analysed in order to deduce several fundamental properties of snake robot dynamics. Some of these properties will be instrumental in the development of a *simplified* model of the snake robot in Chap. 6, where we propose a model that captures only the 'essential' part of the dynamics of the complex model. In Part II of this book, which considers snake robot locomotion in cluttered environments, the complex model will be extended to include contact forces from external obstacles in the environment around the snake robot.

The chapter is organised as follows. The relation between this chapter and previous literature is briefly discussed in Sect. 2.1. Section 2.2 introduces some basic notation that will be used throughout the book. The parameters that characterise the snake robot are presented in Sect. 2.3. The kinematics of the snake robot is described in Sect. 2.4, while two different ground friction models are presented in Sect. 2.5. The model of the snake robot dynamics is presented in Sect. 2.6, is partitioned into an actuated and an unactuated part in Sect. 2.7, and is transformed to a simpler form

P. Liljebäck et al., *Snake Robots*, Advances in Industrial Control,
DOI 10.1007/978-1-4471-2996-7_2, © Springer-Verlag London 2013

through partial feedback linearisation in Sect. 2.8. Finally, the chapter is summarised in Sect. 2.9.

2.1 The Relation Between This Chapter and Previous Literature

Mathematical models of planar snake robot dynamics have previously been developed from first principles in Ma (2001), Saito et al. (2002), and the initial form of the model presented in this chapter is developed using the same approach as in these works. The notation and the ground friction models considered in this chapter are, however, different from the works in Ma (2001), Saito et al. (2002). Moreover, the expression for the linear velocity of individual links given in (2.13a) is novel to this work. The two main novel features of the results presented in this chapter in relation to previous literature are the change of coordinates, which enables us to partition the model into an actuated and an unactuated part (see Sect. 2.7), and the subsequent partial feedback linearisation of the model (see Sect. 2.8). Due to the complexity of the nonlinearised model of the snake robot, much of the model analysis presented in Chap. 4 would not have been feasible without the model transformation.

2.2 Basic Notation

The following notation is used throughout this book:

- The operator $\mathrm{sgn}(\cdot)$ produces a vector containing the sign of each individual element of its argument.
- The operator $\mathrm{diag}(\cdot)$ produces a diagonal matrix with each individual element of its argument along its diagonal.
- The sinus and cosine operators, $\sin(\cdot)$ and $\cos(\cdot)$, are vector operators when their argument is a vector and scalar operators when their argument is a scalar value.
- We will use subscript i to denote element i of a vector (see Table 2.1 below). When parameters of the links (joints) of the snake robot are assembled into a vector, we associate element i of this vector with link i (joint i).
- Symbols representing a vector or a matrix are indicated with a bold font.
- The matrix $\mathbf{I}_k$ represents the $k \times k$ identity matrix, and $\mathbf{0}_{i\times j}$ represents the $i \times j$ matrix of zeros.
- A vector related to link i of the snake robot is either expressed in the global coordinate system or in the local coordinate system of the link (see Fig. 2.1). This is indicated by superscript *global* or *link*, i, respectively. If not otherwise specified, a vector with no superscript is expressed in the global coordinate system.

2.3 The Parameters of the Snake Robot

The snake robot consists of N rigid links of length $2l$ interconnected by $N-1$ motorised joints. The width of each link is not considered in the model. All N links

Table 2.1 Parameters that characterise the snake robot

Symbol	Description	Vector
N	The number of links	
l	Half the length of a link	
m	Mass of each link	
J	Moment of inertia of each link	
θ_i	Angle between link i and the global x axis	$\boldsymbol{\theta} \in \mathbb{R}^N$
ϕ_i	Angle of joint i	$\boldsymbol{\phi} \in \mathbb{R}^{N-1}$
(x_i, y_i)	Global coordinates of the CM of link i	$\mathbf{X}, \mathbf{Y} \in \mathbb{R}^N$
(p_x, p_y)	Global coordinates of the CM of the robot	$\mathbf{p} \in \mathbb{R}^2$
u_i	Actuator torque on link i from link $i+1$	$\mathbf{u} \in \mathbb{R}^{N-1}$
u_{i-1}	Actuator torque on link i from link $i-1$	$\mathbf{u} \in \mathbb{R}^{N-1}$
$(f_{R,x,i}, f_{R,y,i})$	Ground friction force on link i	$\mathbf{f}_{R,x}, \mathbf{f}_{R,y} \in \mathbb{R}^N$
$(h_{x,i}, h_{y,i})$	Joint constraint force on link i from link $i+1$	$\mathbf{h}_x, \mathbf{h}_y \in \mathbb{R}^{N-1}$
$-(h_{x,i-1}, h_{y,i-1})$	Joint constraint force on link i from link $i-1$	$\mathbf{h}_x, \mathbf{h}_y \in \mathbb{R}^{N-1}$

have the same mass m and moment of inertia $J = \frac{1}{3}ml^2$. The total mass of the snake robot is therefore Nm. The mass of each link is uniformly distributed so that the link CM (centre of mass) is located at its centre point (at length l from the joint at each side). In the following subsections, the kinematics and dynamics of the snake robot will be modelled in terms of the mathematical symbols described in Table 2.1 and illustrated in Figs. 2.1 and 2.2. We will make use of the following vectors and matrices:

$$\mathbf{A} = \begin{bmatrix} 1 & 1 & & & \\ & \ddots & \ddots & & \\ & & \ddots & \ddots & \\ & & & 1 & 1 \end{bmatrix} \in \mathbb{R}^{(N-1)\times N},$$

$$\mathbf{D} = \begin{bmatrix} 1 & -1 & & & \\ & \ddots & \ddots & & \\ & & \ddots & \ddots & \\ & & & 1 & -1 \end{bmatrix} \in \mathbb{R}^{(N-1)\times N},$$

$$\mathbf{e} = [1, \ldots, 1]^T \in \mathbb{R}^N, \qquad \mathbf{E} = \begin{bmatrix} \mathbf{e} & \mathbf{0}_{N\times 1} \\ \mathbf{0}_{N\times 1} & \mathbf{e} \end{bmatrix} \in \mathbb{R}^{2N\times 2},$$

$$\sin\boldsymbol{\theta} = [\sin\theta_1, \ldots, \sin\theta_N]^T \in \mathbb{R}^N, \qquad \mathbf{S}_\theta = \operatorname{diag}(\sin\boldsymbol{\theta}) \in \mathbb{R}^{N\times N},$$

$$\cos\boldsymbol{\theta} = [\cos\theta_1, \ldots, \cos\theta_N]^T \in \mathbb{R}^N, \qquad \mathbf{C}_\theta = \operatorname{diag}(\cos\boldsymbol{\theta}) \in \mathbb{R}^{N\times N},$$

$$\operatorname{sgn}\boldsymbol{\theta} = [\operatorname{sgn}\theta_1, \ldots, \operatorname{sgn}\theta_N]^T \in \mathbb{R}^N, \qquad \dot{\boldsymbol{\theta}}^2 = \left[\dot{\theta}_1^2, \ldots, \dot{\theta}_N^2\right]^T \in \mathbb{R}^N.$$

The matrices $\mathbf{A}$ and $\mathbf{D}$ represent, respectively, an *addition* and a *difference* matrix, which will be used, respectively, for adding and subtracting pairs of adjacent ele-

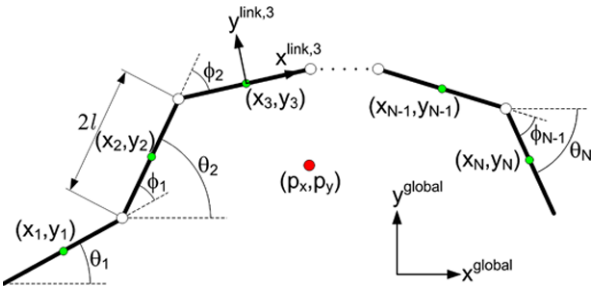

Fig. 2.1 The kinematic parameters of the snake robot

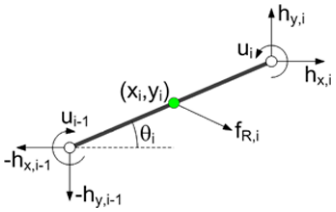

Fig. 2.2 Forces and torques acting on each link of the snake robot

ments of a vector. Furthermore, the vector **e** represents a summation vector, which will be used for adding all elements of an N-dimensional vector. The remaining vectors and matrices have been defined above since they appear several times during the development of the model.

2.4 The Kinematics of the Snake Robot

The snake robot moves on a horizontal and flat surface, and has $N + 2$ degrees of freedom (N link angles and the planar position of the robot). The following definitions are illustrated in Fig. 2.1.

Definition 2.1 (Link angle) The *link angle* of link $i \in \{1, \ldots, N\}$ of the snake robot is denoted by $\theta_i \in \mathbb{R}$ and is defined as the angle that the link forms with the global x axis with counterclockwise positive direction.

Definition 2.2 (Joint angle) The *joint angle* of joint $i \in \{1, \ldots, N-1\}$ of the snake robot is denoted $\phi_i \in \mathbb{R}$ and is defined as

$$\phi_i = \theta_i - \theta_{i+1}. \tag{2.1}$$

Note the distinction between *link angles* and *joint angles*. A link angle is the orientation of a link with respect to the global x axis, while a joint angle is the difference between the link angles of two neighbouring links. We will quite frequently assemble the link angles and the joint angles in the vectors $\boldsymbol{\theta} = [\theta_1, \ldots, \theta_N]^T \in \mathbb{R}^N$ and $\boldsymbol{\phi} = [\phi_1, \ldots, \phi_{N-1}]^T \in \mathbb{R}^{N-1}$, respectively.

The snake robot has no explicitly defined orientation since there is an independent link angle associated with each link. We can still obtain a measure of the heading of the robot as follows (this approach is also considered in e.g. Hatton and Choset 2009a; Hu et al. 2009):

Definition 2.3 (Heading) The *heading* (or *orientation*) of the snake robot is denoted by $\overline{\theta} \in \mathbb{R}$ and is defined as the average of the link angles, i.e. as

$$\overline{\theta} = \frac{1}{N} \sum_{i=1}^{N} \theta_i. \tag{2.2}$$

The local coordinate system of each link is fixed in the CM of the link with x (tangential) and y (normal) axes oriented such that they are aligned with the global x and y axis, respectively, when the link angle is zero. The rotation matrix from the global frame to the frame of link i is given by

$$\mathbf{R}_{\text{link},i}^{\text{global}} = \begin{bmatrix} \cos\theta_i & -\sin\theta_i \\ \sin\theta_i & \cos\theta_i \end{bmatrix}. \tag{2.3}$$

The global frame position $\mathbf{p} \in \mathbb{R}^2$ of the CM (centre of mass) of the robot is given by

$$\mathbf{p} = \begin{bmatrix} p_x \\ p_y \end{bmatrix} = \begin{bmatrix} \frac{1}{Nm} \sum_{i=1}^{N} m x_i \\ \frac{1}{Nm} \sum_{i=1}^{N} m y_i \end{bmatrix} = \frac{1}{N} \begin{bmatrix} \mathbf{e}^T \mathbf{X} \\ \mathbf{e}^T \mathbf{Y} \end{bmatrix}, \tag{2.4}$$

where $\mathbf{e}$ was defined in Sect. 2.3, (x_i, y_i) are the global frame coordinates of the CM of link i, $\mathbf{X} = [x_1, \ldots, x_N]^T \in \mathbb{R}^N$, and $\mathbf{Y} = [y_1, \ldots, y_N]^T \in \mathbb{R}^N$. We define the velocity of the snake robot along its *forward* direction as follows:

Definition 2.4 (Forward velocity) The *forward velocity* of the snake robot is denoted by $\overline{v}_t \in \mathbb{R}$ and is defined as the component of the CM velocity $\dot{\mathbf{p}}$ along the current heading $\overline{\theta}$, i.e. as

$$\overline{v}_t = \dot{p}_x \cos\overline{\theta} + \dot{p}_y \sin\overline{\theta}. \tag{2.5}$$

Remark 2.1 Subscript t in the forward velocity $\overline{v}_t$ denotes *tangential*. The simplified model of the snake robot presented in Chap. 6 makes a clear distinction between the forward velocity v_t and the sideways velocity v_n of the robot. We have chosen to denote the forward velocity in the complex model by $\overline{v}_t$ to maintain a similar notation as in the simplified model.

The connection between link i and link $i+1$ at joint $i \in \{1, \ldots, N-1\}$ must comply with the two *holonomic* constraints

$$x_{i+1} - x_i = l\cos\theta_i + l\cos\theta_{i+1}, \tag{2.6a}$$

$$y_{i+1} - y_i = l\sin\theta_i + l\sin\theta_{i+1}. \tag{2.6b}$$

Using the notation from Sect. 2.3, we can write the joint constraints for all the links of the robot in matrix form as

$$\mathbf{DX} + l\mathbf{A}\cos\boldsymbol{\theta} = \mathbf{0}, \tag{2.7a}$$

$$\mathbf{DY} + l\mathbf{A}\sin\boldsymbol{\theta} = \mathbf{0}. \tag{2.7b}$$

We can now express the position of the individual links as a function of the CM position and the link angles of the robot by combining (2.4) and (2.7a)–(2.7b) into

$$\begin{aligned} \mathbf{TX} &= \begin{bmatrix} -l\mathbf{A}\cos\boldsymbol{\theta} \\ p_x \end{bmatrix}, \\ \mathbf{TY} &= \begin{bmatrix} -l\mathbf{A}\sin\boldsymbol{\theta} \\ p_y \end{bmatrix}, \end{aligned} \tag{2.8}$$

where

$$\mathbf{T} = \begin{bmatrix} \mathbf{D} \\ \frac{1}{N}\mathbf{e}^T \end{bmatrix} \in \mathbb{R}^{N\times N}. \tag{2.9}$$

It can be shown that

$$\mathbf{T}^{-1} = \begin{bmatrix} \mathbf{D}^T\left(\mathbf{DD}^T\right)^{-1} & \mathbf{e} \end{bmatrix}, \tag{2.10}$$

which enables us to solve (2.8) for $\mathbf{X}$ and $\mathbf{Y}$ according to

$$\mathbf{X} = \mathbf{T}^{-1}\begin{bmatrix} -l\mathbf{A}\cos\boldsymbol{\theta} \\ p_x \end{bmatrix} = -l\mathbf{K}^T\cos\boldsymbol{\theta} + \mathbf{e}p_x, \tag{2.11a}$$

$$\mathbf{Y} = \mathbf{T}^{-1}\begin{bmatrix} -l\mathbf{A}\sin\boldsymbol{\theta} \\ p_y \end{bmatrix} = -l\mathbf{K}^T\sin\boldsymbol{\theta} + \mathbf{e}p_y, \tag{2.11b}$$

where $\mathbf{K} = \mathbf{A}^T(\mathbf{DD}^T)^{-1}\mathbf{D} \in \mathbb{R}^{N\times N}$, and where $\mathbf{DD}^T$ is nonsingular and thereby invertible. The linear velocities of the links are found by differentiating (2.11a) and (2.11b) with respect to time, which gives

$$\dot{\mathbf{X}} = l\mathbf{K}^T\mathbf{S}_\theta\dot{\boldsymbol{\theta}} + \mathbf{e}\dot{p}_x, \tag{2.12a}$$

$$\dot{\mathbf{Y}} = -l\mathbf{K}^T\mathbf{C}_\theta\dot{\boldsymbol{\theta}} + \mathbf{e}\dot{p}_y. \tag{2.12b}$$

By manually investigating the structure of each row in (2.12a) and (2.12b), it can be verified that the linear velocity of the CM of link i in the global x and y directions is given by

$$\dot{x}_i = \dot{p}_x - \sigma_i\mathbf{S}_\theta\dot{\boldsymbol{\theta}}, \tag{2.13a}$$

$$\dot{y}_i = \dot{p}_y + \sigma_i\mathbf{C}_\theta\dot{\boldsymbol{\theta}}, \tag{2.13b}$$

where

$$\sigma_i = \left[a_1, a_2, \ldots, a_{i-1}, \frac{a_i + b_i}{2}, b_{i+1}, b_{i+2}, \ldots, b_N \right] \in \mathbb{R}^N, \tag{2.14a}$$

$$a_i = \frac{l(2i-1)}{N}, \qquad b_i = \frac{l(2i-1-2N)}{N}. \tag{2.14b}$$

2.5 The Ground Friction Models

2.5.1 The Friction Models and Their Role in This Book

As will become apparent in Chap. 4, a planar snake robot achieves forward propulsion on a flat surface by continuously changing its body shape to induce ground friction forces that propel the robot forward. The ground friction model is therefore an important part of the dynamics of the snake robot.

During planar locomotion, it is of great advantage to the propulsion of the snake robot that the ground friction forces on the links are *anisotropic*, which means that the friction coefficient describing the friction force in the tangential direction of a link (parallel to the link, i.e. along link x axis) is different from the friction coefficient describing the friction force in the direction normal to the link (perpendicular to the link, i.e. along link y axis). This friction property is exhibited by biological snakes, as was explained in the description of biological snakes in Sect. 1.2, and is also assumed in the majority of published research on snake robots, as described in the literature review of Sect. 1.3. We therefore include anisotropic friction conditions in the friction model of the snake robot. The importance of this friction property will be investigated in more detail in Chap. 4.

Note that anisotropic ground friction properties are typically implemented by mounting passive wheels along the body of the snake robot, but can also be achieved by equipping the underside of each link of the robot with edges, or grooves, that run parallel to each link (see e.g. Saito et al. 2002). If a snake robot does *not* have anisotropic ground friction properties, which is the case if the ground friction force on each link is independent of the link orientation with respect to its direction of motion, the links are said to have *isotropic* ground friction properties. This will typically be the case when the links of the snake robot are completely smooth in all directions. Note also that a snake robot with a completely smooth outer surface will still have anisotropic "friction" properties when it is swimming under water due to the higher drag forces in the direction normal to each link compared to in the tangential link direction (see e.g. Boyer et al. 2006; McIsaac and Ostrowski 2003a).

We consider two different ground friction models in this book, i.e. a *Coulomb* friction model and a *viscous* friction model. The Coulomb friction model, which assumes that the ground friction force on a link is proportional to the weight of the link, is more accurate (from a physical point of view) than the viscous friction model, which assumes that the ground friction force on a link is proportional to the velocity

of the link. However, during planar locomotion, we conjecture that the anisotropic friction property of the links, which is independent of the choice of Coulomb or viscous friction, is the decisive factor of the motion. In other words, we conjecture that the motion of the snake robot is *qualitatively* (although not *quantitatively*) similar with anisotropic viscous friction as with anisotropic Coulomb friction. The viscous friction model is, however, less complex than the Coulomb friction model, which makes the viscous model more suitable for control design and analysis purposes. In this book, we will therefore mostly assume that the ground friction is viscous.

In the following, we first present the Coulomb friction model and subsequently the viscous friction model. In both models, the ground friction force on link i is assumed to act on the CM of the link only and is denoted by

$$\mathbf{f}_{R,i} = \mathbf{f}_{R,i}^{\text{global}} = \begin{bmatrix} f_{R,x,i} \\ f_{R,y,i} \end{bmatrix} \in \mathbb{R}^2. \tag{2.15}$$

The friction forces on all links are written in matrix form as

$$\mathbf{f}_R = \begin{bmatrix} \mathbf{f}_{R,x} \\ \mathbf{f}_{R,y} \end{bmatrix} \in \mathbb{R}^{2N}, \tag{2.16}$$

where $\mathbf{f}_{R,x} = [f_{R,x,1}, \ldots, f_{R,x,N}]^T \in \mathbb{R}^N$ and $\mathbf{f}_{R,y} = [f_{R,y,1}, \ldots, f_{R,y,N}]^T \in \mathbb{R}^N$ contain the friction forces on the links in the global x and y directions, respectively.

2.5.2 A Coulomb Friction Model

The coefficients describing the Coulomb friction force in the tangential (along link x axis) and normal (along link y axis) directions of a link, respectively, are denoted by μ_t and μ_n, respectively. We define the Coulomb friction force on link i in the local link frame, $\mathbf{f}_{R,i}^{\text{link},i} \in \mathbb{R}^2$, as

$$\mathbf{f}_{R,i}^{\text{link},i} = -mg \begin{bmatrix} \mu_t & 0 \\ 0 & \mu_n \end{bmatrix} \text{sgn}\big(\mathbf{v}_i^{\text{link},i}\big), \tag{2.17}$$

where $\mathbf{v}_i^{\text{link},i} \in \mathbb{R}^2$ is the link velocity expressed in the local link frame, and g is the gravitational acceleration constant. Using (2.3), we can express the global frame Coulomb friction force on link i in the form of (2.15) as

$$\begin{aligned} \mathbf{f}_{R,i} &= \mathbf{f}_{R,i}^{\text{global}} = \mathbf{R}_{\text{link},i}^{\text{global}} \mathbf{f}_{R,i}^{\text{link},i} \\ &= -mg \mathbf{R}_{\text{link},i}^{\text{global}} \begin{bmatrix} \mu_t & 0 \\ 0 & \mu_n \end{bmatrix} \text{sgn}\big(\mathbf{v}_i^{\text{link},i}\big) \\ &= -mg \mathbf{R}_{\text{link},i}^{\text{global}} \begin{bmatrix} \mu_t & 0 \\ 0 & \mu_n \end{bmatrix} \text{sgn}\left(\big(\mathbf{R}_{\text{link},i}^{\text{global}}\big)^T \begin{bmatrix} \dot{x}_i \\ \dot{y}_i \end{bmatrix} \right). \end{aligned} \tag{2.18}$$

By performing the matrix multiplication in (2.18) and assembling the forces on all links in matrix form, we can rewrite the global frame Coulomb friction forces on the links in the form of (2.16) as

$$\mathbf{f}_R = \begin{bmatrix} \mathbf{f}_{R,x} \\ \mathbf{f}_{R,y} \end{bmatrix} = -mg \begin{bmatrix} \mu_t \mathbf{C}_\theta & -\mu_n \mathbf{S}_\theta \\ \mu_t \mathbf{S}_\theta & \mu_n \mathbf{C}_\theta \end{bmatrix} \operatorname{sgn}\left(\begin{bmatrix} \mathbf{C}_\theta & \mathbf{S}_\theta \\ -\mathbf{S}_\theta & \mathbf{C}_\theta \end{bmatrix} \begin{bmatrix} \dot{\mathbf{X}} \\ \dot{\mathbf{Y}} \end{bmatrix} \right) \in \mathbb{R}^{2N}. \quad (2.19)$$

2.5.3 A Viscous Friction Model

Similar to the Coulomb friction model, we assume that the viscous ground friction forces act on the CM of the links only. We present the viscous friction model for the different cases of isotropic versus anisotropic viscous friction since these two cases are analysed separately in Chap. 4.

Isotropic Viscous Friction

The isotropic viscous friction force on link i in the global x and y directions is proportional to the global frame velocity of the link given by (2.13a) and (2.13b), and is written in the form of (2.15) as

$$\mathbf{f}_{R,i} = \mathbf{f}_{R,i}^{\text{global}} = -c \begin{bmatrix} \dot{x}_i \\ \dot{y}_i \end{bmatrix} = -c \begin{bmatrix} \dot{p}_x - \sigma_i \mathbf{S}_\theta \dot{\boldsymbol{\theta}} \\ \dot{p}_y + \sigma_i \mathbf{C}_\theta \dot{\boldsymbol{\theta}} \end{bmatrix}, \quad (2.20)$$

where c is the viscous friction coefficient. The friction forces on all links are easily expressed in the form of (2.16) as

$$\mathbf{f}_R = \begin{bmatrix} \mathbf{f}_{R,x} \\ \mathbf{f}_{R,y} \end{bmatrix} = -c \begin{bmatrix} \dot{\mathbf{X}} \\ \dot{\mathbf{Y}} \end{bmatrix} = -c \begin{bmatrix} l\mathbf{K}^T \mathbf{S}_\theta \dot{\boldsymbol{\theta}} + \mathbf{e}\dot{p}_x \\ -l\mathbf{K}^T \mathbf{C}_\theta \dot{\boldsymbol{\theta}} + \mathbf{e}\dot{p}_y \end{bmatrix}, \quad (2.21)$$

where we have used the expression for the link velocities given by (2.12a) and (2.12b).

Anisotropic Viscous Friction

Under anisotropic friction conditions, a link has two viscous friction coefficients, c_t and c_n, describing the friction force in the tangential (along link x axis) and normal (along link y axis) directions of the link, respectively. We define the viscous friction force on link i in the local link frame, $\mathbf{f}_{R,i}^{\text{link},i} \in \mathbb{R}^2$, as

$$\mathbf{f}_{R,i}^{\text{link},i} = -\begin{bmatrix} c_t & 0 \\ 0 & c_n \end{bmatrix} \mathbf{v}_i^{\text{link},i}, \quad (2.22)$$

where $\mathbf{v}_i^{\text{link},i} \in \mathbb{R}^2$ is the link velocity expressed in the local link frame. Using (2.3), we can express the global frame viscous friction force on link i in the form of (2.15) as

$$\begin{aligned}\mathbf{f}_{R,i} &= \mathbf{f}_{R,i}^{\text{global}} = \mathbf{R}_{\text{link},i}^{\text{global}} \mathbf{f}_{R,i}^{\text{link},i} \\ &= -\mathbf{R}_{\text{link},i}^{\text{global}} \begin{bmatrix} c_t & 0 \\ 0 & c_n \end{bmatrix} \mathbf{v}_i^{\text{link},i} \\ &= -\mathbf{R}_{\text{link},i}^{\text{global}} \begin{bmatrix} c_t & 0 \\ 0 & c_n \end{bmatrix} \left(\mathbf{R}_{\text{link},i}^{\text{global}}\right)^T \begin{bmatrix} \dot{x}_i \\ \dot{y}_i \end{bmatrix}. \end{aligned} \tag{2.23}$$

By performing the matrix multiplication in (2.23), we get

$$\mathbf{f}_{R,i} = -\begin{bmatrix} c_t \cos^2\theta_i + c_n \sin^2\theta_i & (c_t - c_n)\sin\theta_i \cos\theta_i \\ (c_t - c_n)\sin\theta_i \cos\theta_i & c_t \sin^2\theta_i + c_n \cos^2\theta_i \end{bmatrix} \begin{bmatrix} \dot{x}_i \\ \dot{y}_i \end{bmatrix}. \tag{2.24}$$

By assembling the forces on all links in matrix form, we can rewrite the global frame viscous friction forces on the links in the form of (2.16) as

$$\mathbf{f}_R = \begin{bmatrix} \mathbf{f}_{R,x} \\ \mathbf{f}_{R,y} \end{bmatrix} = -\begin{bmatrix} c_t(\mathbf{C}_\theta)^2 + c_n(\mathbf{S}_\theta)^2 & (c_t - c_n)\mathbf{S}_\theta \mathbf{C}_\theta \\ (c_t - c_n)\mathbf{S}_\theta \mathbf{C}_\theta & c_t(\mathbf{S}_\theta)^2 + c_n(\mathbf{C}_\theta)^2 \end{bmatrix} \begin{bmatrix} \dot{\mathbf{X}} \\ \dot{\mathbf{Y}} \end{bmatrix} \in \mathbb{R}^{2N}. \tag{2.25}$$

Note that (2.25) reduces to (2.21) in the case of isotropic friction, i.e. where $c_t = c_n = c$.

2.6 The Dynamics of the Snake Robot

The $N + 2$ degrees of freedom of the snake robot are defined by the link angles $\boldsymbol{\theta} \in \mathbb{R}^N$ and the CM position $\mathbf{p} \in \mathbb{R}^2$. We now present the equations of motion of the robot in terms of the acceleration of the link angles, $\ddot{\boldsymbol{\theta}}$, and the acceleration of the CM position, $\ddot{\mathbf{p}}$.

As illustrated in Fig. 2.2, link $i \in \{1, \ldots, N\}$ is influenced by the ground friction force $\mathbf{f}_{R,i} \in \mathbb{R}^2$, which acts on the CM of the link, and also the joint constraint forces $-h_{x,i-1}$, $-h_{y,i-1}$, $h_{x,i}$, and $h_{y,i}$, which keep the link connected to link $i - 1$ and link $i + 1$. The joint constraint forces are described in Table 2.1. Using first principles, the force balance for link i in global frame coordinates is given by

$$m\ddot{x}_i = f_{R,x,i} + h_{x,i} - h_{x,i-1}, \tag{2.26a}$$

$$m\ddot{y}_i = f_{R,y,i} + h_{y,i} - h_{y,i-1}. \tag{2.26b}$$

The force balance equations for all links may be expressed in matrix form as

$$m\ddot{\mathbf{X}} = \mathbf{f}_{R,x} + \mathbf{D}^T \mathbf{h}_x, \tag{2.27a}$$

$$m\ddot{\mathbf{Y}} = \mathbf{f}_{R,y} + \mathbf{D}^T \mathbf{h}_y, \tag{2.27b}$$

where $\mathbf{h}_x = [h_{x,1}, \ldots, h_{x,N}]^T \in \mathbb{R}^N$ and $\mathbf{h}_y = [h_{y,1}, \ldots, h_{y,N}]^T \in \mathbb{R}^N$. The link accelerations may also be expressed by differentiating (2.7a) and (2.7b) twice with respect to time, which gives

$$\mathbf{D}\ddot{\mathbf{X}} = l\mathbf{A}\big(\mathbf{C}_\theta \dot{\boldsymbol{\theta}}^2 + \mathbf{S}_\theta \ddot{\boldsymbol{\theta}}\big), \tag{2.28a}$$

$$\mathbf{D}\ddot{\mathbf{Y}} = l\mathbf{A}\big(\mathbf{S}_\theta \dot{\boldsymbol{\theta}}^2 - \mathbf{C}_\theta \ddot{\boldsymbol{\theta}}\big), \tag{2.28b}$$

where the square operator of $\dot{\boldsymbol{\theta}}^2$ means that each element of $\dot{\boldsymbol{\theta}}$ is squared ($\dot{\boldsymbol{\theta}}^2 = \text{diag}(\dot{\boldsymbol{\theta}})\dot{\boldsymbol{\theta}}$). We obtain the CM acceleration by differentiating (2.4) twice with respect to time, inserting (2.27a) and (2.27b), and noting that the joint constraint forces, $\mathbf{h}_x$ and $\mathbf{h}_y$, are eliminated when the link accelerations are summed (i.e. $\mathbf{e}^T\mathbf{D}^T = \mathbf{0}$). This gives

$$\begin{bmatrix} \ddot{p}_x \\ \ddot{p}_y \end{bmatrix} = \frac{1}{N}\begin{bmatrix} \mathbf{e}^T\ddot{\mathbf{X}} \\ \mathbf{e}^T\ddot{\mathbf{Y}} \end{bmatrix} = \frac{1}{Nm}\begin{bmatrix} \mathbf{e}^T\mathbf{f}_{R,x} \\ \mathbf{e}^T\mathbf{f}_{R,y} \end{bmatrix} = \frac{1}{Nm}\mathbf{E}^T\mathbf{f}_R. \tag{2.29}$$

This equation simply states, as would be expected, that the acceleration of the CM of the snake robot equals the sum of the external forces acting on the robot divided by its mass.

The torque balance for link i is given by

$$J\ddot{\theta}_i = u_i - u_{i-1} - l\sin\theta_i(h_{x,i} + h_{x,i-1}) + l\cos\theta_i(h_{y,i} + h_{y,i-1}), \tag{2.30}$$

where u_i and u_{i-1} are the actuator torques exerted on link i from link $i+1$ and link $i-1$, respectively. Hence, the torque balance equations for all links may be expressed in matrix form as

$$J\ddot{\boldsymbol{\theta}} = \mathbf{D}^T\mathbf{u} - l\mathbf{S}_\theta\mathbf{A}^T\mathbf{h}_x + l\mathbf{C}_\theta\mathbf{A}^T\mathbf{h}_y. \tag{2.31}$$

It now remains to remove the joint constraint forces from (2.31). Premultiplying (2.27a) and (2.27b) by $\mathbf{D}$, solving for $\mathbf{h}_x$ and $\mathbf{h}_y$, and also inserting (2.28a) and (2.28b) give

$$\mathbf{h}_x = \big(\mathbf{D}\mathbf{D}^T\big)^{-1}\big(ml\mathbf{A}\big(\mathbf{C}_\theta\dot{\boldsymbol{\theta}}^2 + \mathbf{S}_\theta\ddot{\boldsymbol{\theta}}\big) - \mathbf{D}\mathbf{f}_{R,x}\big), \tag{2.32a}$$

$$\mathbf{h}_y = \big(\mathbf{D}\mathbf{D}^T\big)^{-1}\big(ml\mathbf{A}\big(\mathbf{S}_\theta\dot{\boldsymbol{\theta}}^2 - \mathbf{C}_\theta\ddot{\boldsymbol{\theta}}\big) - \mathbf{D}\mathbf{f}_{R,y}\big). \tag{2.32b}$$

By inserting (2.32a) and (2.32b) into (2.31) and solving for $\ddot{\boldsymbol{\theta}}$, we can finally rewrite the model of the snake robot as

$$\mathbf{M}_\theta\ddot{\boldsymbol{\theta}} + \mathbf{W}\dot{\boldsymbol{\theta}}^2 - l\mathbf{S}_\theta\mathbf{K}\mathbf{f}_{R,x} + l\mathbf{C}_\theta\mathbf{K}\mathbf{f}_{R,y} = \mathbf{D}^T\mathbf{u}, \tag{2.33a}$$

$$Nm\ddot{\mathbf{p}} = Nm\begin{bmatrix} \ddot{p}_x \\ \ddot{p}_y \end{bmatrix} = \begin{bmatrix} \mathbf{e}^T\mathbf{f}_{R,x} \\ \mathbf{e}^T\mathbf{f}_{R,y} \end{bmatrix} = \mathbf{E}^T\mathbf{f}_R, \tag{2.33b}$$

where $\mathbf{f}_R$ is either the Coulomb friction force given by (2.19) or the viscous friction force given by (2.25), and where

$$\mathbf{M}_\theta = J\mathbf{I}_N + ml^2\mathbf{S}_\theta\mathbf{V}\mathbf{S}_\theta + ml^2\mathbf{C}_\theta\mathbf{V}\mathbf{C}_\theta, \tag{2.34a}$$

$$\mathbf{W} = ml^2\mathbf{S}_\theta\mathbf{V}\mathbf{C}_\theta - ml^2\mathbf{C}_\theta\mathbf{V}\mathbf{S}_\theta, \tag{2.34b}$$

$$\mathbf{V} = \mathbf{A}^T\left(\mathbf{D}\mathbf{D}^T\right)^{-1}\mathbf{A}, \tag{2.34c}$$

$$\mathbf{K} = \mathbf{A}^T\left(\mathbf{D}\mathbf{D}^T\right)^{-1}\mathbf{D}. \tag{2.34d}$$

By introducing the state variable $\mathbf{x} = [\boldsymbol{\theta}^T, \mathbf{p}^T, \dot{\boldsymbol{\theta}}^T, \dot{\mathbf{p}}^T]^T \in \mathbb{R}^{2n+4}$, we can rewrite the model of the snake robot compactly in state space form as

$$\dot{\mathbf{x}} = \begin{bmatrix} \dot{\boldsymbol{\theta}} \\ \dot{\mathbf{p}} \\ \ddot{\boldsymbol{\theta}} \\ \ddot{\mathbf{p}} \end{bmatrix} = \mathbf{F}(\mathbf{x}, \mathbf{u}), \tag{2.35}$$

where the elements of $\mathbf{F}(\mathbf{x}, \mathbf{u})$ are easily found by solving (2.33a) and (2.33b) for $\ddot{\boldsymbol{\theta}}$ and $\ddot{\mathbf{p}}$, respectively.

2.7 Separating Actuated and Unactuated Dynamics

The model of the snake robot in (2.33a) and (2.33b) is rather complex for analysis and control design purposes. We therefore seek a transformation which allows us to write the model in a simpler form. Partial feedback linearisation of underactuated systems (see e.g. Gu and Xu 1993; Spong 1994) consists of linearising the dynamics corresponding to the actuated degrees of freedom of the system. We will employ this methodology in the next section. However, before partial feedback linearisation can be carried out, the model of the snake robot in (2.33a) and (2.33b) must be partitioned into two parts representing the actuated and unactuated degrees of freedom, respectively. This partitioning is now carried out.

The acceleration of the CM of the snake robot, $\ddot{\mathbf{p}}$, belongs to the unactuated part since it is not directly influenced by the input, $\mathbf{u}$. The acceleration of the link angles, $\ddot{\boldsymbol{\theta}}$, represents one unactuated degree of freedom and $N-1$ actuated degrees of freedom since there are N link accelerations ($\boldsymbol{\theta} \in \mathbb{R}^N$) and only $N-1$ control inputs ($\mathbf{u} \in \mathbb{R}^{N-1}$). However, it is not possible to partition the equation for $\ddot{\boldsymbol{\theta}}$ in (2.33a) into an actuated and an unactuated part since the matrix $\mathbf{D}^T$ in front of the control input gives a direct influence between $\mathbf{u}$ and all the link accelerations. We therefore seek a form of the model where there is a direct influence between $\mathbf{u}$ and only $N-1$ link accelerations. This is achieved by modifying the choice of generalised coordinates from absolute link angles to relative joint angles. The generalised coordinates of the model in (2.33a) and (2.33b) are given by the link angles, $\boldsymbol{\theta}$, and the CM position of the snake robot, $\mathbf{p}$. We now replace these coordinates with

$$\mathbf{q}_\phi = \begin{bmatrix} \boldsymbol{\phi} \\ \mathbf{p} \end{bmatrix} \in \mathbb{R}^{N+2}, \tag{2.36}$$

where $\overline{\boldsymbol{\phi}} = [\phi_1, \ldots, \phi_{N-1}, \theta_N]^T \in \mathbb{R}^N$ contains the $N-1$ joint angles of the snake robot and the absolute link angle, $\theta_N \in \mathbb{R}$, of the head link . The joint angles were defined in Definition 2.2. The coordinate transformation between link angles and joint angles is easily shown to be given by

$$\boldsymbol{\theta} = \mathbf{H}\overline{\boldsymbol{\phi}}, \quad \mathbf{H} = \begin{bmatrix} 1 & 1 & 1 & \cdots & 1 & 1 \\ 0 & 1 & 1 & \cdots & 1 & 1 \\ \vdots & & & & & \vdots \\ 0 & 0 & 0 & \cdots & 0 & 1 \end{bmatrix} \in \mathbb{R}^{N \times N}. \tag{2.37}$$

The model of the snake robot in the new coordinates is found by inserting (2.37) into (2.33a). This gives

$$\mathbf{M}_\theta \mathbf{H}\ddot{\overline{\boldsymbol{\phi}}} + \mathbf{W}\,\mathrm{diag}(\mathbf{H}\dot{\overline{\boldsymbol{\phi}}})\mathbf{H}\dot{\overline{\boldsymbol{\phi}}} - l\mathbf{S}_\theta \mathbf{K}\mathbf{f}_{R,x} + l\mathbf{C}_\theta \mathbf{K}\mathbf{f}_{R,y} = \mathbf{D}^T\mathbf{u}, \tag{2.38a}$$

$$Nm\ddot{\mathbf{p}} = \mathbf{E}^T\mathbf{f}_R, \tag{2.38b}$$

where we have used that $\dot{\boldsymbol{\theta}}^2 = \mathrm{diag}(\dot{\boldsymbol{\theta}})\dot{\boldsymbol{\theta}} = \mathrm{diag}(\mathbf{H}\dot{\overline{\boldsymbol{\phi}}})\mathbf{H}\dot{\overline{\boldsymbol{\phi}}}$. Finally, we premultiply (2.38a) with $\mathbf{H}^T$ in order to achieve the desired form of the input mapping matrix on the right-hand side by making the last of the N equations independent of the control input. This enables us to write the complete model of the snake robot as

$$\overline{\mathbf{M}}(\overline{\boldsymbol{\phi}})\ddot{\mathbf{q}}_\phi + \overline{\mathbf{W}}(\overline{\boldsymbol{\phi}}, \dot{\overline{\boldsymbol{\phi}}}) + \overline{\mathbf{G}}(\overline{\boldsymbol{\phi}})\mathbf{f}_R(\overline{\boldsymbol{\phi}}, \dot{\overline{\boldsymbol{\phi}}}, \dot{\mathbf{p}}) = \overline{\mathbf{B}}\mathbf{u}, \tag{2.39}$$

where

$$\mathbf{q}_\phi = \begin{bmatrix} \overline{\boldsymbol{\phi}} \\ \mathbf{p} \end{bmatrix}, \tag{2.40a}$$

$$\overline{\mathbf{M}}(\overline{\boldsymbol{\phi}}) = \begin{bmatrix} \mathbf{H}^T\mathbf{M}_\theta(\overline{\boldsymbol{\phi}})\mathbf{H} & \mathbf{0}_{N\times 2} \\ \mathbf{0}_{2\times N} & Nm\mathbf{I}_2 \end{bmatrix}, \tag{2.40b}$$

$$\overline{\mathbf{W}}(\overline{\boldsymbol{\phi}}, \dot{\overline{\boldsymbol{\phi}}}) = \begin{bmatrix} \mathbf{H}^T\mathbf{W}(\overline{\boldsymbol{\phi}})\,\mathrm{diag}(\mathbf{H}\dot{\overline{\boldsymbol{\phi}}})\mathbf{H}\dot{\overline{\boldsymbol{\phi}}} \\ \mathbf{0}_{2\times 1} \end{bmatrix}, \tag{2.40c}$$

$$\overline{\mathbf{G}}(\boldsymbol{\phi}) = \begin{bmatrix} -l\mathbf{H}^T\mathbf{S}_{H\overline{\phi}}\mathbf{K} & l\mathbf{H}^T\mathbf{C}_{H\overline{\phi}}\mathbf{K} \\ -\mathbf{e}^T & \mathbf{0}_{1\times N} \\ \mathbf{0}_{1\times N} & -\mathbf{e}^T \end{bmatrix}, \tag{2.40d}$$

$$\overline{\mathbf{B}} = \begin{bmatrix} \mathbf{I}_{N-1} \\ \mathbf{0}_{3\times(N-1)} \end{bmatrix}, \tag{2.40e}$$

and where $\mathbf{S}_{H\overline{\phi}} = \mathbf{S}_\theta$ and $\mathbf{C}_{H\overline{\phi}} = \mathbf{C}_\theta$.

Remark 2.2 It is interesting to note that premultiplying (2.38a) with $\mathbf{H}^T$ both causes the input mapping matrix $\overline{\mathbf{B}}$ to attain a desirable form and produces a symmetrical inertia matrix $\overline{\mathbf{M}}$. Had we left the model in the form of (2.38a) and (2.38b), the inertia matrix would not have been symmetrical.

The first $N-1$ equations of (2.39) represent the dynamics of the relative joint angles of the snake robot, i.e. the *actuated* degrees of freedom of the snake robot. The last three equations represent the dynamics of the absolute orientation and position of the snake robot, i.e. the *unactuated* degrees of freedom. The model may therefore be partitioned as

$$\overline{\mathbf{M}}_{11}\ddot{\mathbf{q}}_a + \overline{\mathbf{M}}_{12}\ddot{\mathbf{q}}_u + \overline{\mathbf{W}}_1 + \overline{\mathbf{G}}_1\mathbf{f}_R = \mathbf{u}, \tag{2.41a}$$

$$\overline{\mathbf{M}}_{21}\ddot{\mathbf{q}}_a + \overline{\mathbf{M}}_{22}\ddot{\mathbf{q}}_u + \overline{\mathbf{W}}_2 + \overline{\mathbf{G}}_2\mathbf{f}_R = \mathbf{0}_{3\times 1}, \tag{2.41b}$$

where $\mathbf{q}_a = [\phi_1, \ldots, \phi_{N-1}]^T \in \mathbb{R}^{N-1}$ represents the actuated degrees of freedom, $\mathbf{q}_u = [\theta_N, p_x, p_y]^T \in \mathbb{R}^3$ represents the unactuated degrees of freedom, $\overline{\mathbf{M}}_{11} \in \mathbb{R}^{(N-1)\times(N-1)}$, $\overline{\mathbf{M}}_{12} \in \mathbb{R}^{(N-1)\times 3}$, $\overline{\mathbf{M}}_{21} \in \mathbb{R}^{3\times(N-1)}$, $\overline{\mathbf{M}}_{22} \in \mathbb{R}^{3\times 3}$, $\overline{\mathbf{W}}_1 \in \mathbb{R}^{N-1}$, $\overline{\mathbf{W}}_2 \in \mathbb{R}^3$, $\overline{\mathbf{G}}_1 \in \mathbb{R}^{(N-1)\times 2N}$, and $\overline{\mathbf{G}}_2 \in \mathbb{R}^{3\times 2N}$.

Remark 2.3 $\overline{\mathbf{M}}(\overline{\boldsymbol{\phi}})$ only depends on the relative joint angles of the snake robot and not on the absolute orientation of the head link, θ_N. Formally, this is a result of the fact that θ_N is a *cyclic* coordinate (Goldstein et al. 2002). Less formally, this is quite obvious since it would not be reasonable that the inertial properties of a planar snake robot be dependent on how the snake robot is oriented in the plane. We therefore have that $\overline{\mathbf{M}} = \overline{\mathbf{M}}(\mathbf{q}_a)$.

2.8 Partial Feedback Linearisation of the Model

Based on the partitioned model in (2.41a) and (2.41b), we are now ready to transform the model of the snake robot to a simpler form through partial feedback linearisation (see Gu and Xu 1993; Spong 1994) by introducing an input transformation which linearises the dynamics of the actuated degrees of freedom in (2.41a). This conversion greatly simplifies the controllability and stabilisability analysis of the snake robot presented in Chap. 4. We will follow the approach presented in Reyhanoglu et al. (1999).

We begin by solving (2.41b) for $\ddot{\mathbf{q}}_u$ as

$$\ddot{\mathbf{q}}_u = -\overline{\mathbf{M}}_{22}^{-1}(\overline{\mathbf{M}}_{21}\ddot{\mathbf{q}}_a + \overline{\mathbf{W}}_2 + \overline{\mathbf{G}}_2\mathbf{f}_R), \tag{2.42}$$

where $\overline{\mathbf{M}}_{22}$ is an invertible 3×3 matrix as a consequence of the uniform positive definiteness of the system inertia matrix $\overline{\mathbf{M}}(\mathbf{q}_a)$. Inserting (2.42) into (2.41a) gives

$$\big(\overline{\mathbf{M}}_{11} - \overline{\mathbf{M}}_{12}\overline{\mathbf{M}}_{22}^{-1}\overline{\mathbf{M}}_{21}\big)\ddot{\mathbf{q}}_a + \overline{\mathbf{W}}_1 + \overline{\mathbf{G}}_1\mathbf{f}_R - \overline{\mathbf{M}}_{12}\overline{\mathbf{M}}_{22}^{-1}(\overline{\mathbf{W}}_2 + \overline{\mathbf{G}}_2\mathbf{f}_R) = \mathbf{u}. \tag{2.43}$$

Consequently, the following linearising controller

$$\mathbf{u} = \big(\overline{\mathbf{M}}_{11} - \overline{\mathbf{M}}_{12}\overline{\mathbf{M}}_{22}^{-1}\overline{\mathbf{M}}_{21}\big)\overline{\mathbf{u}} + \overline{\mathbf{W}}_1 + \overline{\mathbf{G}}_1\mathbf{f}_R - \overline{\mathbf{M}}_{12}\overline{\mathbf{M}}_{22}^{-1}(\overline{\mathbf{W}}_2 + \overline{\mathbf{G}}_2\mathbf{f}_R), \tag{2.44}$$

where $\overline{\mathbf{u}} = [\overline{u}_1, \ldots, \overline{u}_{N-1}]^T \in \mathbb{R}^{N-1}$ is a new set of control inputs, enables us to rewrite (2.41a) and (2.41b) as

$$\ddot{\mathbf{q}}_a = \overline{\mathbf{u}}, \tag{2.45a}$$

$$\ddot{\mathbf{q}}_u = \mathcal{A}(\mathbf{q}_\phi, \dot{\mathbf{q}}_\phi) + \mathcal{B}(\mathbf{q}_a)\overline{\mathbf{u}}, \tag{2.45b}$$

where

$$\mathcal{A}(\mathbf{q}_\phi, \dot{\mathbf{q}}_\phi) = -\overline{\mathbf{M}}_{22}^{-1}(\overline{\mathbf{W}}_2 + \overline{\mathbf{G}}_2\mathbf{f}_R) \in \mathbb{R}^3, \tag{2.46a}$$

$$\mathcal{B}(\mathbf{q}_a) = -\overline{\mathbf{M}}_{22}^{-1}\overline{\mathbf{M}}_{21} \in \mathbb{R}^{3\times(N-1)}. \tag{2.46b}$$

This model may be written in the standard form of a control-affine system by defining $\mathbf{x}_1 = \mathbf{q}_a$, $\mathbf{x}_2 = \mathbf{q}_u$, $\mathbf{x}_3 = \dot{\mathbf{q}}_a$, $\mathbf{x}_4 = \dot{\mathbf{q}}_u$, and $\mathbf{x} = [\mathbf{x}_1^T, \mathbf{x}_2^T, \mathbf{x}_3^T, \mathbf{x}_4^T]^T \in \mathbb{R}^{2N+4}$. This gives

$$\dot{\mathbf{x}} = \begin{bmatrix} \dot{\mathbf{x}}_1 \\ \dot{\mathbf{x}}_2 \\ \dot{\mathbf{x}}_3 \\ \dot{\mathbf{x}}_4 \end{bmatrix} = \begin{bmatrix} \mathbf{x}_3 \\ \mathbf{x}_4 \\ \overline{\mathbf{u}} \\ \mathcal{A}(\mathbf{x}) + \mathcal{B}(\mathbf{x}_1)\overline{\mathbf{u}} \end{bmatrix} = \mathbf{f}(\mathbf{x}) + \sum_{j=1}^{N-1} \big(\mathbf{g}_j(\mathbf{x}_1)\overline{u}_j\big), \tag{2.47}$$

where

$$\mathbf{f}(\mathbf{x}) = \begin{bmatrix} \mathbf{x}_3 \\ \mathbf{x}_4 \\ \mathbf{0}_{(N-1)\times 1} \\ \mathcal{A}(\mathbf{x}) \end{bmatrix}, \qquad \mathbf{g}_j(\mathbf{x}_1) = \begin{bmatrix} \mathbf{0}_{(N-1)\times 1} \\ \mathbf{0}_{3\times 1} \\ \mathbf{e}_j \\ \mathcal{B}_j(\mathbf{x}_1) \end{bmatrix}, \tag{2.48}$$

$j \in \{1, \ldots, N-1\}$, $\mathbf{e}_j$ denotes the jth standard basis vector in $\mathbb{R}^{N-1}$ (the jth column of $\mathbf{I}_{N-1}$), and $\mathcal{B}_j(\mathbf{x}_1)$ denotes the jth column of $\mathcal{B}(\mathbf{x}_1)$. In literature that considers control-affine systems, the vector $\mathbf{f}(\mathbf{x})$ is often called the drift vector field, while the vectors $\mathbf{g}_j(\mathbf{x}_1)$ are called the control vector fields.

Remark 2.4 We have used $\mathbf{x}$ to denote the state vector of the model (2.47) and also the state vector of the model (2.35) even though these two state vectors are not identical (the difference being the use of joint angles in (2.47) and link angles in (2.35)). Several models of snake robot locomotion are presented in this book, the presentation of which would be obscured by the introduction of a new symbol to represent the state vector of each model. Since the various models are treated separately, which means that it will always be clear from the context which elements that are contained in the state $\mathbf{x}$, we choose to denote the state vector in all models by $\mathbf{x}$.

Remark 2.5 The input transformation in (2.44) is nonsingular, which means that results from analysis and control design based on the partially linearised model in (2.47) are also applicable to the nonlinearised model in (2.35). This is obvious since the behaviour of the model in (2.47) with a control law for $\overline{\mathbf{u}}$ is identical to the behaviour of the model in (2.35) with the control law for $\overline{\mathbf{u}}$ transformed to $\mathbf{u}$ according to (2.44).

2.9 Chapter Summary

This chapter is summarised as follows:

- We have presented a mathematical model of a planar snake robot with N rigid links interconnected by $N-1$ motorised joints. The surface underneath the robot was assumed to be flat and horizontal.
- We have developed two different ground friction models, i.e. a Coulomb friction model given by (2.19) and a viscous friction model given by (2.25).
- The equations of motion of the snake robot in terms of the acceleration of the link angles, $\ddot{\boldsymbol{\theta}}$, and the acceleration of the CM position, $\ddot{\mathbf{p}}$, are given by (2.33a) and (2.33b).
- The equations of motion of the snake robot in terms of the acceleration of the joint angles, $\ddot{\boldsymbol{\phi}}$, the acceleration of the head link angle, $\ddot{\theta}_N$, and the acceleration of the CM position, $\ddot{\mathbf{p}}$, are given by (2.41a) and (2.41b). In this model, the *actuated* degrees of freedom of the snake robot are separated from the *unactuated* degrees of freedom.
- With the input transformation in (2.44), the model of the snake robot is partially feedback linearised to the simpler form given by (2.47). This form is more suitable for control design and analysis purposes.

http://www.springer.com/978-1-4471-2995-0

Snake Robots
Modelling, Mechatronics, and Control
Liljebäck, P.; Pettersen, K.Y.; Stavdahl, O.; Gravdahl, J.T.
2013, XVII, 317 p. 124 illus., 122 illus. in color.,
Hardcover
ISBN: 978-1-4471-2995-0